Electronic Supplementary Material (ESI) for Nanoscale.

Supplementary Information

Highly Stretchable Strain Sensors with Reduced Graphene Oxide Sensing Liquids for Wearable Electronics

Minxuan Xu, Junjie Qi, Feng Li, Yue Zhang**

State Key Laboratory for Advanced Metals and Materials, School of Materials Science and Engineering, University of Science and Technology Beijing, Beijing 100083, China

***Corresponding authors, E-mail: junjieqi@ustb.edu.cn**

yuezhang@ustb.edu.cn

Table of contents

1. Materials and Methods

2. Supplementary Table

3. Supplementary Figures

4. Mechanism Analysis

5. Supplementary References

1. Materials and Methods

Material: The $KMnO_4$, H_2SO_4 (98%), H_3PO_4 (85%), H_2O_2 (30%), HCl (37%), N_2H_4-H_2O (≥85%) and NH_3-H_2O (≥25%) were purchased from Sinopharm Chemical Reagent Co., Ltd. Natural graphite flakes (325 meshes) was provided by Alfa-Aesar. The Ecoflex rubber (00-30) was provided by Smooth-On and the acrylic tape (3mm thick, 4965PV0) was purchased from TESA. All these reagents were used without further purification.

Preparation of GO: GO was synthesized by the oxidation of 325 meshes graphite flakes based on the modified Hummers method. [1] Typically, natural graphite flakes (3.0 g) was dispersed in a mixture of concentrated H_2SO_4/H_3PO_4 (360:40 ml) under stirring in an ice bath, $KMnO_4$ (18 g) was added slowly to keep the temperature of the suspension lower than 20℃. Then, the reaction system was transferred to a 40℃ oil bath and vigorously stirred for about 30 min. Then, 50 ml deionized water (DI) was added, stirred for another 15 min at 95℃. Successively, additional 150 ml water was added, and 5 ml H_2O_2 was added drop wise until gas generation was completed, turning the color of the solution from dark brown to yellow. Bright-yellow suspension was treated by filtration, and the resulting solid material was washed 3 times with 1:9 HCl aqueous solutions (50 ml) to remove metal ions, and then, washed with DI to remove the residual acid. Finally, the resulting solid GO was dried in air and dispersed in DI to form 0.5 mg/ml GO aqueous dispersion for use.

Preparation of rGO foams: GO dispersion was reduced to rGO according to a previously reported method. [2] The resulting homogeneous GO dispersion (0.5 mg/ml, 50 ml) was mixed with 50 ml DI, 17.5 μl N_2H_4-H_2O and 350 μl NH_3-H_2O in a 250-ml reaction flask. After being vigorously stirred for a few minutes, the reaction system was set in a 95℃ oil bath for 1 h. When the reaction was completed, gauze was used to filter out a small amount of residue. Successively, the as-obtained rGO foams were collected and then diluted to a desired concentration.

Fabrication of rGO/DI liquids strain sensor: The cleaned PET substrate (100μm thick) was cut into size of 40mm×30mm and was patterned in a rectangular shape (30mm×10mm×3mm) with acrylic tape covered around the PET. Then, the rectangular shape was filled up with 2g mixed Ecoflex rubber (mass ratio A: B=1:1) after a wire (d=1mm) was left in the middle. When the rubber was cured after 2 hours, the acrylic tape was detached from the PET slide. The wire was pulled to one end as the conductor and left a cylindrical cavity (30mm long, d=1mm). Another wire (d=1mm) was used to block the cylindrical cavity after the as-obtained rGO/DI liquids injected into. Finally, the translucent and highly

stretchable strain sensor (30mm×10mm×3mm) was manufactured after sealing and peeling off the PET. The length of sensing fluid is 20 mm.

Characterizations and testing: The Raman spectrum was obtained by utilizing confocal Raman spectroscopy (Horiba JY-HR800) with an Ar^+ laser source at room temperature (λ=633nm). JEOL scanning electron microscope (SEM, JSM-6490) was employed to observe the morphology of synthesized materials. The electromechanical properties of the strain sensors were measured with semiconductor characterization system (Keithley 4200) and a digital source meter (Keithley DMM-7510).

2. Supplementary Table

Table S1. The performance comparison of strain sensors("-"means Not Shown)

Material	Maximum GF	Stretch ability	Limit of detection	Durability	Reference
Carbon fiber+ZnO NWs	80	1.2%	0.2%	-	*[3]Nanoscale* 2013
rGO foams	5	68%	-	-	*[4]. Adv. Mater.* 2014
CNT	2	80	-	-	*[5] Carbon* 2014
Ag NP	7	20	0.4%	1000	*[6]Nanoscale* 2014
Graphene-Nanocellulose paper	7.1	100%	6%	-	*[7]. Adv. Mater.* 2014
Laser scribed graphene	9.49	18%	0.05%	150	*[8] Nanoscale.* 2014
Ag NWs+elastomer	14	70%	-	-	*[9]ACS Nano* 2014
Au NWs	7.38	25%	-	50000	*[10]Nat. Commun.* 2014
Graphene foam	30	50%	-	1000	*[11]. Small* 2015
Graphite flakes	536.6	0.6%	0.13%	10000	*[12]. Adv. Funct. Mater.* 2015
Graphene foams+PDMS	29	70%	0.25%	10000	*[13]. Adv. Funct. Mater.* 2015
Fiber of compression spring architecture	3.7	100%	0.2%	10000	*[14]. Adv. Mater.* 2015
Graphene mesh fabric on stretchable tape	20	7.5%	-	500	*[15]. ACS Nano* 2015
Nanographene films on PDMS	500	1.6%	0.2%	10000	*[16]. ACS Nano 2015*
Graphene foam+PI	5	70%	-	2000	*[17]. ACS Nano*

					2015
Ag NWs	20	35%	-	-	*[18]. Nano Letter* 2015
Fish scale-like rGO/tape film	16	82%	0.1%	5000	*[19]. ACS Nano 2016*
Self-Assembly Graphene film	228	4.4%	0.25%	-	*[20]. Adv. Funct. Mater.* 2016
MoS_2+Graphene film	50	5%	0.12%	1000	*[21]. Adv. Mater.* 2016
Ag NWs+rubber	4	100%	-	100000	*[22]. Adv. Mater.* 2016
Graphene+TPU foam	12.24	90%	-	50	*[23]. J. Mater. Chem. C.*. 2017
PVA/MWCNT/PEDOT:PSS	5.2	50%	-	10000	*[24]. Nanoscale.* 2017
Graphene foam+CNT	35	85%	-	5000	*[25]. Adv. Mater.* 2017
RGO+DI liquids	**31.6**	**400%**	**0.1%**	**10000**	**This work**

3. Supplementary Figures

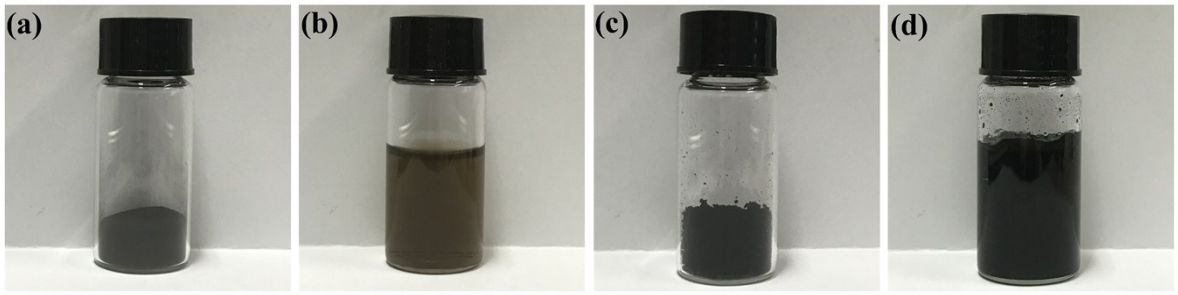

Figure S1. Digital photographs of a) natural graphite flakes, b) GO suspension, c) rGO foams, and d) rGO/DI liquids.

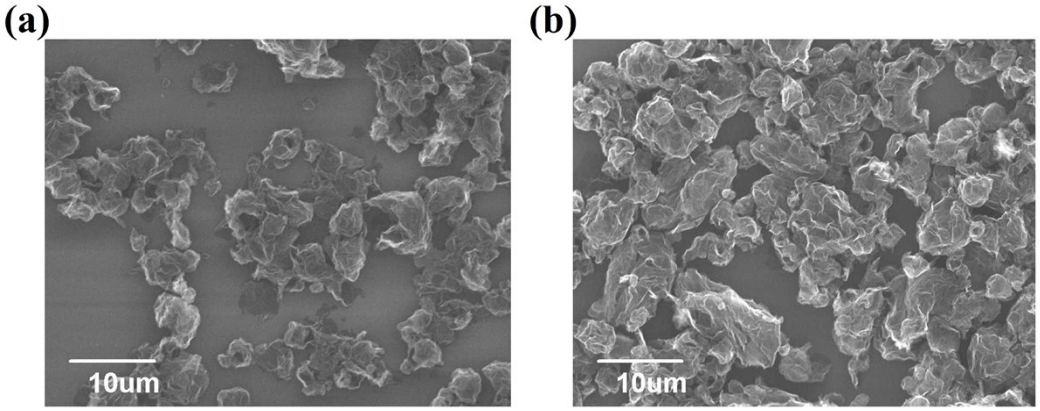

Figure S2. SEM images of rGO foams from rGO/DI liquids a) 1 mg/ml, b) 6 mg/ml.

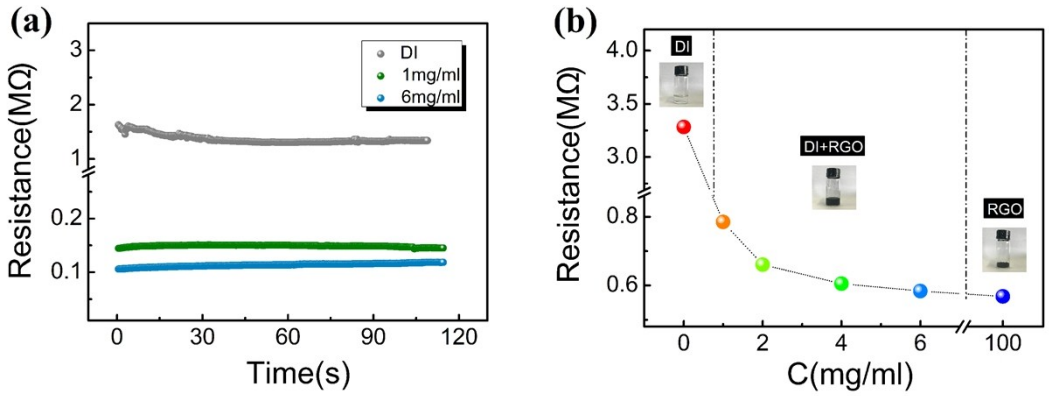

Figure S3. a) Resistance-time curves of DI (2 ml), RGO/DI liquids (1 mg/ml, 6 mg/ml, and 5 ml), b) Resistances of DI (1 ml), rGO/DI liquids (1 ml) and 6 mg pure rGO solid.

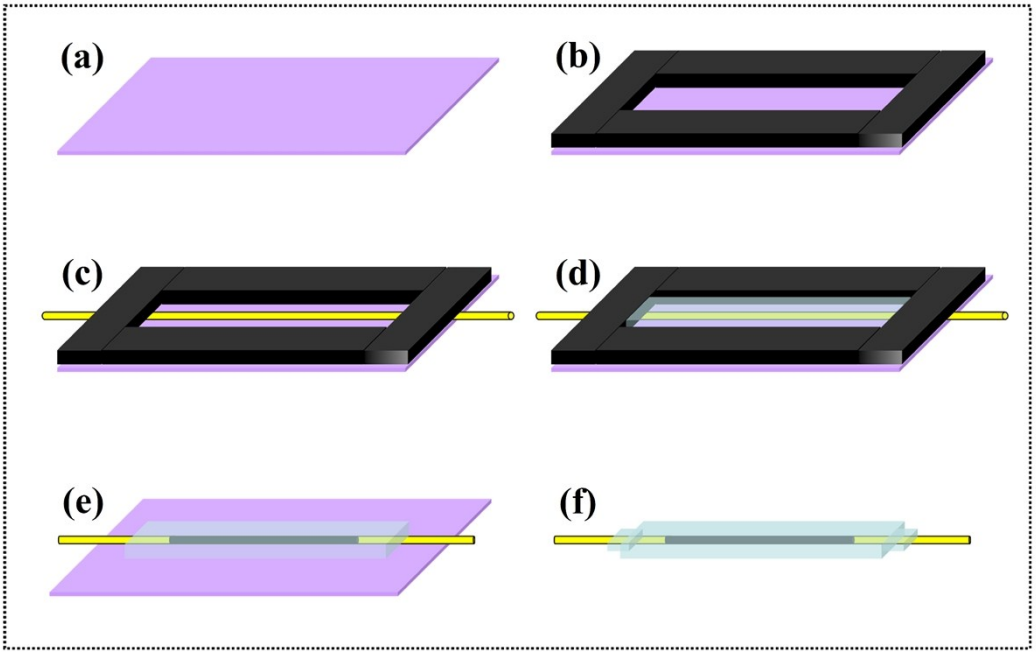

Figure S4. Schematic illustration of fabricating the rGO/DI liquids strain sensor a) PET substrate, b) patterned in a rectangular shape (30 mm×10 mm×3 mm), c) a wire (d=1 mm) was installed above the PET substrate, d) filled up with 2 g mixed Ecoflex rubber and cured after 2 hours, e) filled up with the sensing liquids, f) sealed and peeled off the PET.

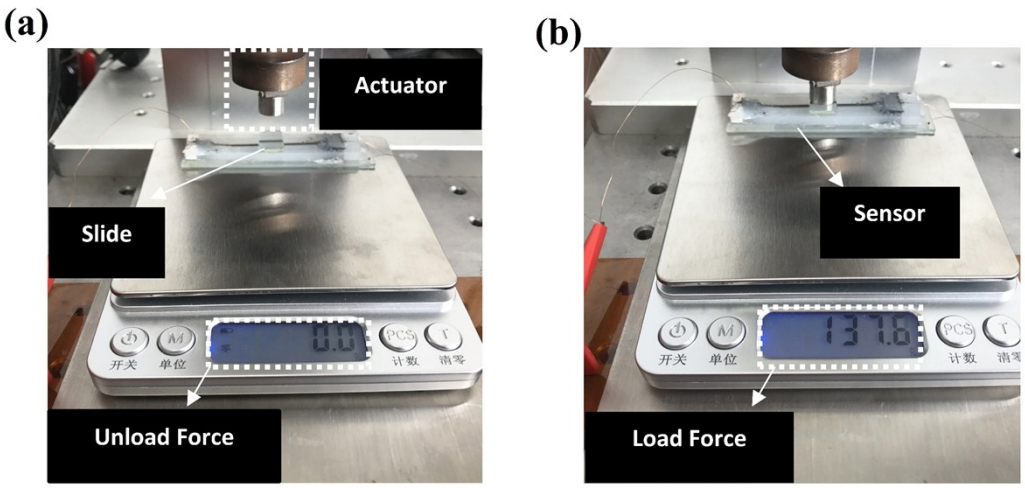

Figure S5. Schematic illustration of the pressure measurement setup a) Unload, b) Load.

The pressure applied in the vertical direction and it can be considered equal to the weight measured by the electronic balance. It means F=mg. The pressure act on the slide (10 mm wide) which was always contacted the upper surface of the device (10 mm wide). Therefore, the pressure acting area is a constant equivalent to the size of the slide (10 mm wide, 15mm long) during the pressure applied.

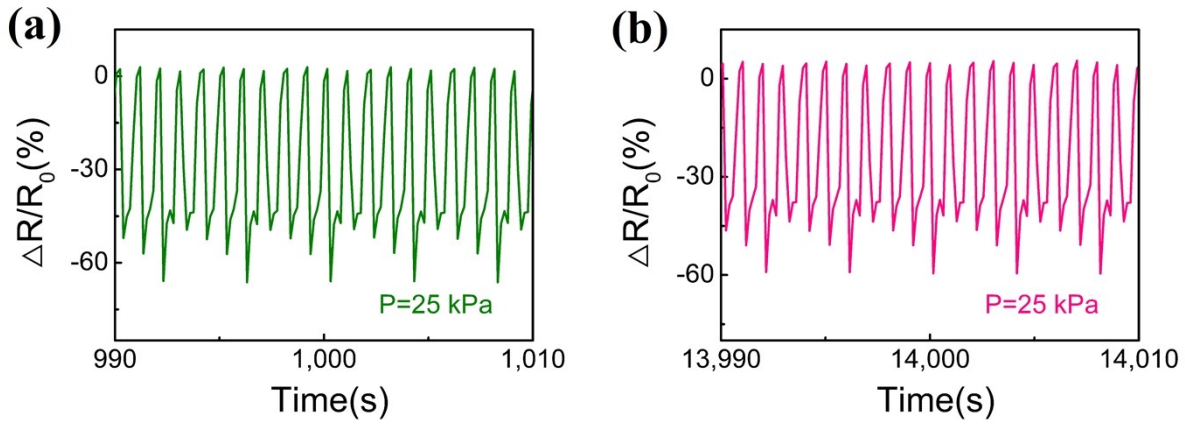

Figure S6. Mechanical stability of cycling pressure rGO/DI liquids strain sensor a) 1000 cycles, b) 14000 cycles.

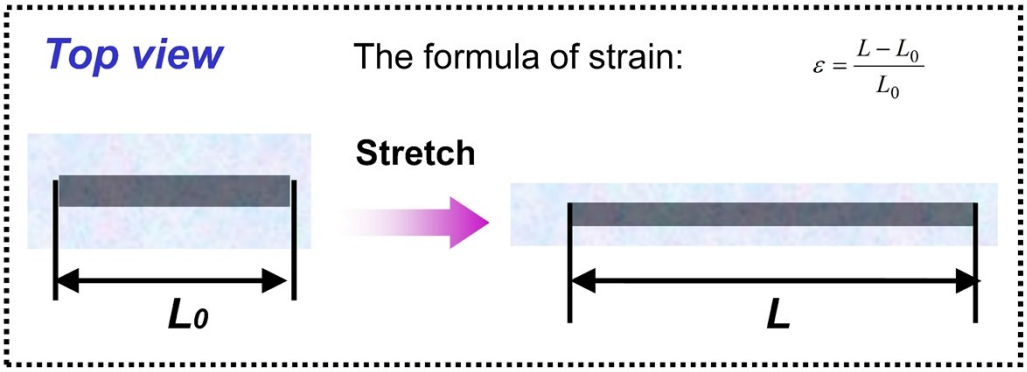

Figure S7. The method of calculating the strain during the stretch applied.

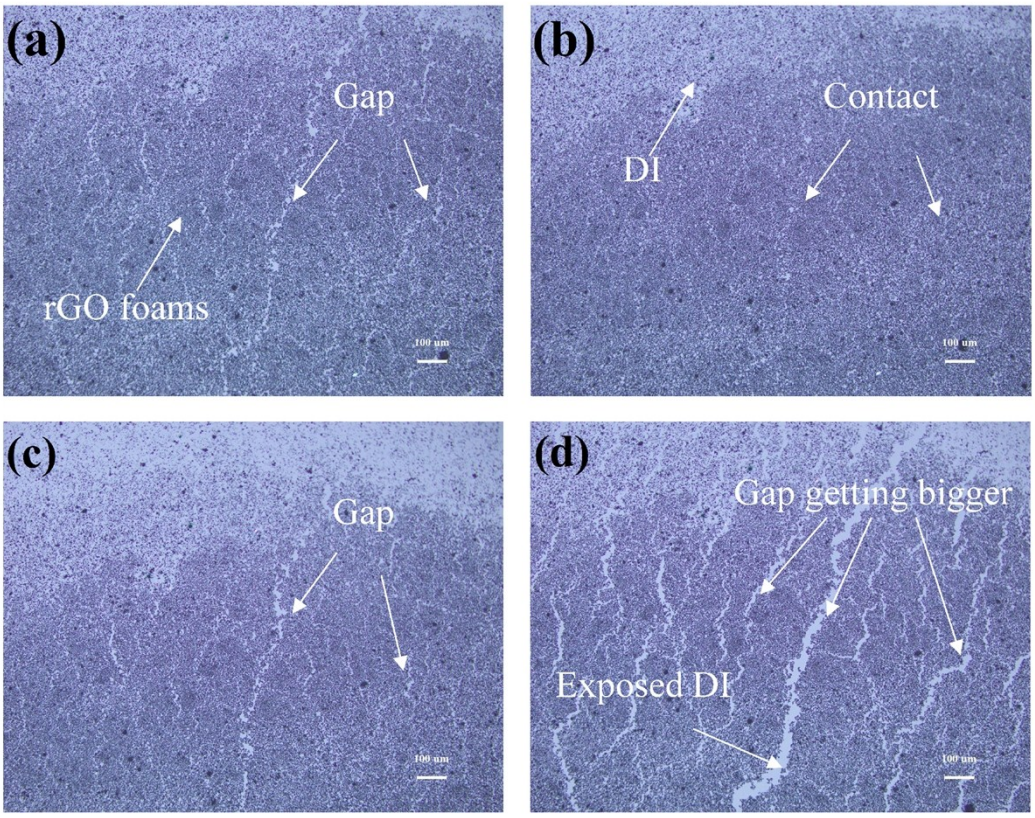

Figure S8. Top-view images of the rGO/DI liquids (6mg/ml) a) Unload, b) Loading with 5 kPa, c) Relax, d) Stretch with 5%.

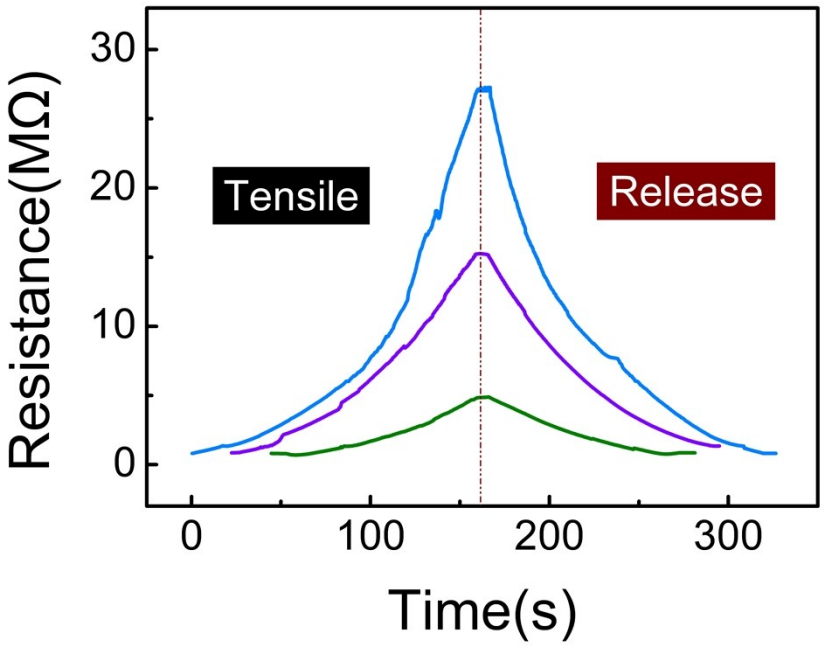

Figure S9. The typical resistance-time curve of the rGO/DI liquids strain sensor upon cyclic stretching/releasing to 200%, 300% and 400% (stretching rate = releasing rate = 2.5 %·s^{-1}).

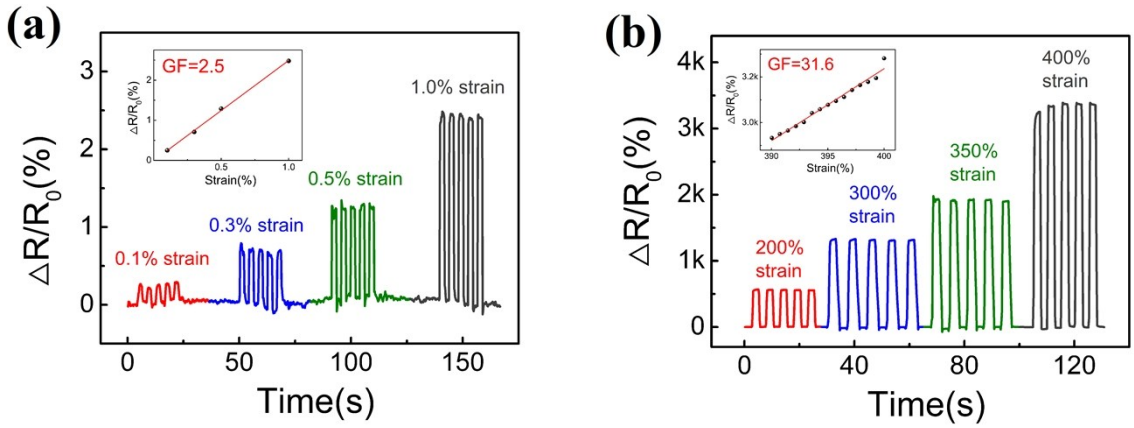

Figure S10. Mechanical stability of cycling tensile rGO/DI liquids strain sensor under a) small strain from 0.1% to 1%, b) large strain from 200% to 400%..

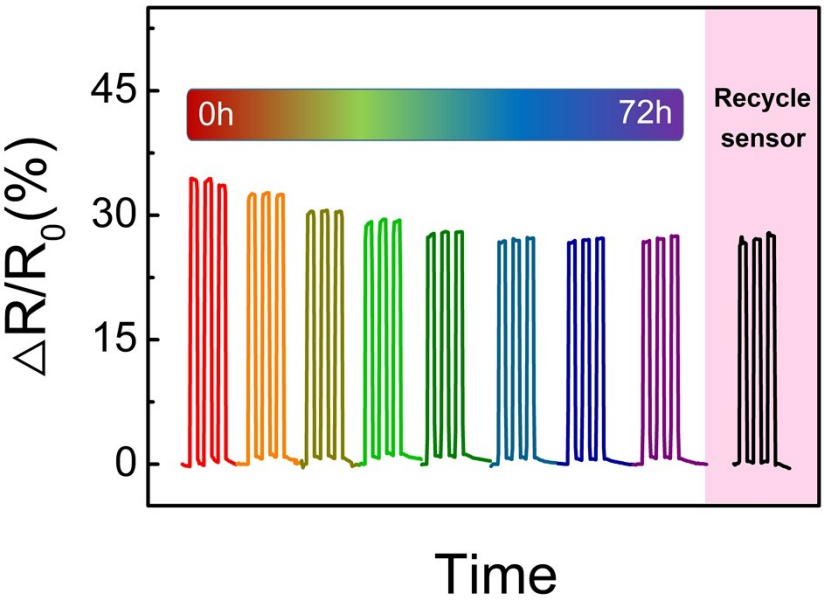

Figure S11. The durability of the sensor over the time from 0 hour to 72 hours after fabrication, and the response curve of the device recycled the sensing liquid.

4. Mechanism Analysis

On the basis of the Figure 2, the sensing mechanism of rGO/DI liquids strain sensor is theoretically analyzed as follows.

The initial resistance of this strain sensor, R_0, can be depicted by equation S1:

$$R_0 = R_D + R_r = \rho \frac{l}{S} + R_r \tag{S1}$$

Where R_D is the inherent resistance of DI, R_r is the contact resistance of rGO foams at 0% strain or 0kPa. There ρ, *l*, *S* is the resistivity, length and cross-sectional area of DI respectively. We reasonably assume R_D is much larger than R_r, based on the Fig. S4 that compared to DI ($10^6\ \Omega$), the resistance of the rGO/DI liquids is closer to the rGO solid ($10^5\ \Omega$).

At a pressure of P, the resistance R is described as:

$$R_p = R_D^{'} + R_r^{'} = \rho \frac{l}{S_1} + R_r^{'} \tag{S2}$$

Where R_r' is the contact resistance of rGO foams at the pressure of P.

The resistance of DI will increase according to the reduce of cross-sectional area ($S \geq S_1$). However the contact resistance of rGO foams will decrease according to micro-contact effect of rGO foams in the liquids. [16] The final change in resistance ΔR is a combination of both. It is believed that the resistance change in R_r is much larger than R_D, based on the Fig. 3c that

the resistance of strain sensor decreased during the pressure applied. The electronic resistance variation ratios ($\Delta R/R_P$) chosen to express the change of current during different pressures in the deformation process is mainly determined by the change of R_r. [26] Therefore, the pressure sensitivity of rGO/DI liquids strain sensor determined by the micro-contact effect of rGO foams in the liquids can be calculated as follows:

$$S = \frac{\delta(\Delta R/R_0)}{\delta P} = \frac{\delta\left[(R_0 - R_P)/R_0\right]}{\delta P} \tag{S3}$$

During the stretching process, the resistance R is described as:

$$R_\varepsilon = R_D^{'} + R_r^{'} = \rho\frac{l_1}{S_1} + R_r^{'} \tag{S2}$$

Where R_r' is the contact resistance of rGO foams at the strain of ε.

Both the DI resistance and the contact resistance will increase because the shape of the sensing liquids becomes slender ($S > S_1$, $l < l_1$). After the sensor being stretched to a strain of ε, the gauge factor (GF) of stretch can be calculated as follow:

$$GF = \frac{\delta(\Delta R/R_0)}{\delta\varepsilon} = \frac{\delta\left[(R_\varepsilon - R_0)/R_0\right]}{\delta\varepsilon} \tag{S5}$$

5. Supplementary References

[1]. J. Chen, B. Yao, C. Li, G. Shi, *Carbon* **2013**, 64, 225.

[2]. D. Li, M. B. Mueller, S. Gilje, R. B. Kaner, G. G. Wallace, *Nat. Nanotechnol*. **2008**, 3, 101.

[3]. Q. L. Liao, M. Mohr, X. H. Zhang, Z. Zhang, Y. Zhang , H.-J. Fecht, *Nanoscale* **2013**, 5, 12350.

[4]. C. Hou, H. Wang, Q. Zhang, Y. Li, M. Zhu, *Adv. Mater*. **2014**, 26, 5018.

[5]. J. Sebastian, N. Schehl, M. Bouchard, M. Boehle, L. Li, A. Lagounov, K. Lafdi, *Carbon*, **2014**, 66, 191.

[6]. J. Lee, S. Kim, J. Lee, D. Yang, B. C. Park, S. Ryu, I. Park, *Nanoscale*, **2014**, 6, 11932.

[7]. C. Yan, J. Wang, W. Kang, M. Cui, X. Wang, C. Foo, K. Chee, P. Lee, *Adv. Mater*. **2014**, 26, 2022.

[8]. H. Tian, Y. Shu, Y.-L. Cui, W.-T. Mi, Y. Yang, D. Xie, T.-L. Ren, *Nanoscale* **2014**, 6, 699.

[9]. M. Amjadi, A. Pichitpajongkit, S. Lee, S. Ryu, I. Park, *ACS Nano* **2014**, 8, 5154.

[10]. S. Gong, W. Schwalb, Y. W. Wang, Y. Chen, Y. Tang, J. Si, B. Shirinzadeh, W. L. Cheng, *Nat. Commun.,* **2014**, 5, 3132.

[11]. Y. Samad, Y. Li, A. Schiffer, S. Alhassan, K. Liao, *Small* **2015**, 11, 2380.

[12]. X. Liao, Q. Liao, X. Yan, Q. Liang, H. Si, M. Li, H. Wu, S. Cao, Y. Zhang, *Adv. Funct. Mater*. **2015**, 25, 2395.

[13]. Y. R. Jeong, H. Park, S. W. Jin, S. Y. Hong, S.-S. Lee, J. S. Ha, *Adv. Funct. Mater*. **2015**, 25, 4228.

[14]. Y. Cheng, R. Wang, J. Sun, L. Gao, *Adv. Mater*. **2015**, 27, 7365.

[15]. Q. Liu, M. Zhang, L. Huang, Y. Li, J. Chen, C. Li, G. Shi, *ACS Nano* **2015**, 9, 12320.

[16]. J. Zhao, G. Wang, R. Yang, X. Lu, M. Cheng, C. He, G. Xie, J. Meng, D. Shi, G. Zhang, *ACS Nano* **2015**, 9, 1622.

[17]. Y. Qin, Q. Peng, Y. Ding, Z. Lin, C. Wang, Y. Li, F. Xu, J. Li, Y. Yuan, X. He, Y. Li, *ACS Nano* **2015**, 9, 8933.

[18]. K. K. Kim, S. Hong, H. M. Cho, J. Lee, Y. D. Suh, J. Ham and S. H. Ko, *Nano Lett.,* **2015**, 15, 5240.

[19]. Q. Liu, J. Chen, Y. Li, G. Shi, *ACS Nano* **2016**, 10, 7901.

[20]. X. Li, T. Yang, Y. Yang, J. Zhu, L. Li, F. E. Alam, X. Li, K. Wang, H. Cheng, C. T. Lin, *Adv. Funct. Mater.* **2016**, 26, 1322

[21]. M. Park, Y. J. Park, X. C, Y.-K. Park, M.-S. Kim, J.-H. Ahn, *Adv. Mater.* **2016**, 28, 2556.

[22]. J. Ge, L. Sun, F. R. Zhang, Y. Zhang, L. A. Shi, H. Y. Zhao, H. W. Zhu, H. L. Jiang and S. H. Yu, *Adv. Mater.*, **2016**, 28, 722.

[23]. H. Liu, M. Y. Dong, W. J. Huang, J. C. Gao, K. Dai, J. Guo, G. Q. Zheng, C. T. Liu, C. Y. Shen, Z. H. Guo, *J. Mater. Chem. C,* **2017**, 5, 73.

[24]. H. Park, D. S. Kim, S. Y. Hong, C. Kim, J. Y. Yun, S. Y. Oh, S. W. Jin, Y. R. Jeong, G. T. Kim, J. S. Ha, *Nanoscale*, **2017**, 9, 7631.

[25]. Y. C. Cai, J. Shen, Z. Y. Dai, X, X. Zang, Q. C. Dong, G. F. Guan, L.-J. Li, W. Huang, X. C. Dong, *Adv. Mater.*, **2017**, 29, 1606411.

[26]. C. Lin, Z. Zhao, J. Kim, J. Huang, *Sci. Rep.* **2014**, 4, 580.